

Cerebrovascular alterations in APP23 transgenic mice modelling Alzheimer's disease studied non-invasively by MRI

N. Beckmann¹, S. Zurbrugg¹, C. Cagnet¹, C. Gérard¹, D. Abramowski², K-H. Wiederhold², and M. Staufenbiel²

¹Global Imaging Group, Novartis Institutes for BioMedical Research, Basel, Switzerland, ²Nervous System Area, Novartis Institutes for BioMedical Research, Basel, Switzerland

Introduction:

Alzheimer's disease (AD) is characterized by amyloid-beta- (A β -) peptide containing plaques, neurofibrillary tangles consisting of aggregated, hyper-phosphorylated tau, extensive neuritic degeneration, and distinct neuron loss. Vascular abnormalities coexist commonly with the histological features of AD. About 80% of AD cases exhibit cerebral amyloid angiopathy (CAA) (1), characterized by deposition of A β peptide in the walls of cerebral vessels. The presence of macrophages in the walls of vessels affected by CAA has been related to the progression of CAA-related microvasculopathy in AD patients (2). Microglia and macrophages surrounding CAA-affected microvessels in the brain parenchyma (3), or circulating monocytes that migrate from the lumen into the vessel wall (2,4) have been shown to contribute to the vascular thickening. In this work, we used superparamagnetic iron oxide (SPIO) particles to detect by MRI CAA-related cerebrovascular changes in APP23 mice (5).

Materials and Methods:

Animals: The generation of APP23 mice containing the murine Thy-1 promoter driving neuron specific expression of human mutated APP751 is described in detail in (5). Studies were carried out on age-matched APP23 and on wildtype littermate, male mice.

MRI: Mice were anesthetized with 1.3 % isoflurane (Abbott, Cham, Switzerland) in a mixture of O₂/N₂O (1:2) administered via a face mask. No stereotactic holding was used. Measurements were carried out with a Biospec 47/40 spectrometer (Bruker, Karlsruhe, Germany) operating at 4.7 T. Images were obtained using a three-dimensional (3D) gradient-echo sequence with the following imaging parameters: TR 40 ms; TE 8 ms; matrix 256x192x48; FOV 2.8x1.44x1.44 cm³, 2 averages. The data sets were reconstructed to (256)³. Acquisitions were performed 24 h after intravenous Endorem injection (0.2 ml).

Image analysis: Images were analyzed by an investigator who was unaware of the genotype and of the age of the mice. Foci in the cortex presenting signal attenuation and a minimum diameter of 150 μ m were counted throughout the whole brain. To ensure that the same site was not counted multiple times, its presence was carefully controlled over several consecutive slices from the 3D data set.

Histology: Performed at the levels of lesions observed by MRI. Hematoxylin and eosin staining was employed to assess the general morphology. The Perls/Prussian blue reaction, the periodic acid-Schiff (PAS) reaction and Congo red were used to visualize ferric iron, pathologic deposits and amyloid, respectively.

Results and Discussion:

Figure 1a shows coronal MR images extracted from 3D data sets acquired from 28-month-old APP23 mice, 24 h after SPIO. Signal attenuations were apparent in multiple foci throughout the brain cortex, as indicated by the arrows, as well as in thalamic regions. No contrast change was detected in the brains of age-matched wildtype controls 24 h following SPIO (figure 1a), with the exception of a few animals displaying scant attenuations in the cortex. Histological analysis revealed that iron was localized in or around damaged vessels at sites of signal loss detected in vivo by MRI in APP23 mice (figure 1b). Iron was encountered in the vessel wall, at the level of amyloid deposits or in the vicinity of pathologic blood vessels, mainly entrapped in microglia cells/macrophages. Since iron was mainly found entrapped in macrophages, it is conceivable that SPIO nanoparticles were absorbed in the blood circulation by monocytes, which then infiltrated the walls of pathologic vessels.

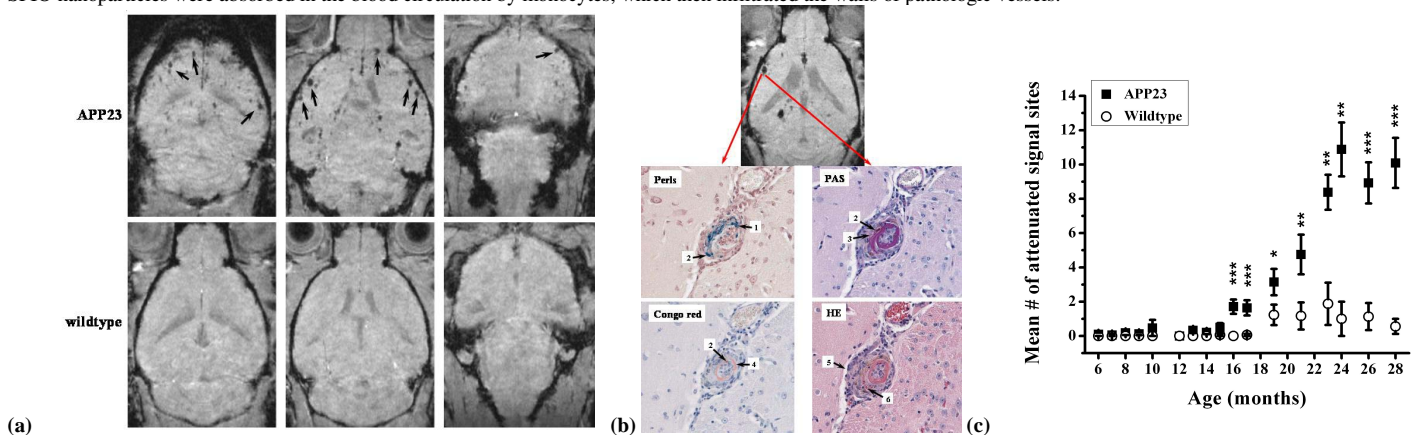


Fig. 1 – (a) Brain images extracted from MRI 3D data sets acquired from 28-month-old mice 24 h after SPIO administration. Foci of signal attenuation (arrows) were detected throughout the cortex of APP23, but not of wildtype animals. **(b)** Histological sections corresponding to the site indicated in the MR image. 1, iron in vessel wall; 2, iron in macrophage/microglia; 3, thickened vessel wall; 4, amyloid deposit in vessel wall; 5, vasculitis; 6, perivascular hemorrhage. **(c)** Number of sites (mean \pm sem) presenting signal attenuation in the brain cortex of male APP23 mice and age-matched littermate controls, determined from 3D MRI data sets. The number of animals analyzed at each time point ranged from 8 to 16. The levels of significance * 0.01 < p < 0.05, ** 0.001 < p < 0.01 or *** 0.0001 < p < 0.001 refer to Mann-Whitney statistical tests performed at the specified ages. SPIO was administered 24 h before each image acquisition.

The number of attenuated signal foci present in the brain cortex is summarized in figure 1c for animals of different ages. This time course is consistent with previous results reported for APP23 mice, showing age-related vascular damage due to neuron-derived cerebrovascular amyloid (6). CAA in APP23 mice leads to a loss of vascular smooth muscle cells, and this weakening of the vessel wall can be followed by rupture and the formation of microhemorrhages (6). Thus, besides accumulation of SPIO in areas comprising pathologic vessels, microhemorrhages might have contributed to the localized signal losses in our MR images. Under our acquisition conditions, images of old APP23 animals acquired without any contrast agent administration showed only a small number of attenuated signal sites, which could be potentially related to microbleedings.

The present observations demonstrate that MRI in combination with the administration of SPIO is an important tool to study CAA in transgenic mice modeling AD. These results thus support the idea that cerebral microcirculatory abnormalities evolving progressively could contribute to AD pathogenesis.

1. Jellinger KA. J Neural Transm 2002; 109:813-836.
 3. Maat-Schieman MLC et al. J Neuropathol Exp Neurol 1997; 56:273-284.
 5. Sturchler-Pierrat C et al. Proc Natl Acad Sci USA 1997; 94:13287-13292.

2. Vinters HV. Stroke 1987; 18:311-324.
 4. Vinters HV et al. Acta Neuropathol (Berl) 1998; 95:235-244.
 6. Winkler DT et al. J Neurosci 2001; 21:1619-1627.